Ophthalmic Research

Research Article

Ophthalmic Res 2022;65:685–697
DOI: 10.1159/000525584

Received: January 18, 2022
Accepted: May 22, 2022
Published online: July 14, 2022

The Link between Anterior Scleral Thickness, Corneal Biomechanical Response, and Ocular Parameters

Neus Burguera-Giménez[a, b] M. Amparo Díez-Ajenjo[a, b] Noemí Burguera[c]
M. José Luque-Cobija[a, b] Cristina Peris-Martínez[a, d]

[a]Anterior Segment and Cornea and External Eye Diseases Unit, FISABIO-Oftalmología Médica (FOM), Valencia, Spain; [b]Department of Optics and Optometry and Vision Sciences, Physics School, University of Valencia, Valencia, Spain; [c]Ophthalmology Department, Qvision, Vithas Virgen Del Mar Hospital, Almería, Spain; [d]Surgery Department, Ophthalmology, School of Medicine, University of Valencia, Valencia, Spain

Keywords
Anterior scleral thickness · Biomechanical corneal response · Swept-source optical coherence tomography

Abstract

Introduction: This study aimed to assess anterior scleral thickness (AST) across diverse scleral meridians and to evaluate the relationship with corneal biomechanical response and several ocular parameters. ***Methods:*** This prospective nonrandomized study comprised 50 eyes of 50 patients (mean age, 29.02 ± 9.48 years). AST was measured meridionally at three scleral locations (1, 2, and 3 mm posterior to the scleral spur) using swept-source optical coherence tomography. A multivariate model was created to associate AST with several ocular parameters. Principal component analysis (PCA) was used to reduce linearly the dimensionality of seven biomechanical input metrics to two significant components, C1 and C2. Two multivariate analyses were performed to associate C1 and C2 with AST and ocular parameters. ***Results:*** AST was thickest in the inferior (581 ± 52 μm) and thinnest in the superior meridian (441 ± 42 μm) when compared to all meridians ($p < 0.001$) and similar in the nasal (529 ± 53 μm) and temporal (511 ± 59 μm) meridians ($p > 0.05$). The sclera exhibited the thinnest point 2 mm posterior to the scleral spur ($p < 0.001$). The AST was significantly linked with axial length, central corneal thickness, and intraocular pressure ($p < 0.001$). The PCA showed that C1 accounts for 53.84%, whereas C2 for the 16.51% of the total variance in the original variables. The C1 model was significantly associated with AST along all meridians ($p < 0.001$). The partial correlation was moderate in the nasal ($r = -0.36$, $p < 0.001$) and inferior ($r = -0.26$, $p = 0.004$) meridians, whereas weak in the temporal ($r = -0.14$, $p = 0.05$) and superior ($r = -0.15$, $p = 0.05$) meridians. ***Conclusions:*** The relationship between the new biomechanical component and the AST provides the first evidence of the association of AST with the corneal response parameters which should be considered in corneal response interpretation. Tissue thickness varied significantly among meridians supporting the asymmetrical expansion of the ocular globe. The AST was associated with several ocular parameters.

Karger@karger.com
www.karger.com/ore

Correspondence to:
Neus Burguera-Giménez, neus.burguera@uv.es

Introduction

The cornea and the sclera are the two outer coats of connective tissue that are responsible for maintaining and supporting the proper structure of the eye and balance the outward push intraocular pressure (IOP) [1–3]. The sclera comprises around 85% of the ocular shell, and its principal composition is water, collagen fibers, proteoglycans, and glycoproteins [1]. The scleral interwoven lamellae and the heterogenous collagen distribution provide greater stiffness than corneal tissue, where the fibril organizations are homogeneous, uniform, and highly structured [4].

Several studies have associated collagen distribution with tissue biomechanical behavior [1, 2, 5], which plays a central role in monitoring pathologies. It is known that the alteration of corneal structural properties has an effect on IOP measurements [6–8] and on corneal response, which has proved to be a potential screening tool in the initial ectatic stages, when morphological changes come about [9, 10]. However, it has recently been suggested that corneal biomechanics could also be affected by the boundary structures, like the sclera. Metzler et al. [11] demonstrated that corneal deformation was reduced with stiffer surrounding structures due to the higher resistance to fluid displacement, limiting the corneal response. Likewise, Nguyen et al. [12, 13] described the existence of a corneoscleral interaction with an air puff pulse and also proved that variable scleral stiffness could be a limitation in corneal deformation that could have clinical implications in its interpretation.

It has been widely reported that IOP and pachymetry are the most influential parameters in the biomechanical corneal metrics [14–16]. However, given the growing evidence of the role of boundary structures, the interaction between both connective tissues, and the influence of scleral elasticity in the dynamic biomechanical response, led us to postulate that anterior scleral thickness (AST) could be associated with biomechanical corneal features.

AST has been studied by several authors to determine if factors, such as myopia [2, 17, 18], axial length (AL) [19, 20], central corneal thickness (CCT) [21], accommodation [22], convergence [23], and keratoconus [24], are related to scleral thickness. Other researchers focused on diurnal and aging scleral-thickness variations [25, 26]. More recently, Fernandez-Vigo et al. [27] assessed the correlation of AST with many ocular parameters and revealed associations with various anterior segment parameters. Nearly all the studies agreed about the association between AL and AST. However, there is no general consensus regarding the impact of aging, gender, refractive error, CCT, and IOP.

It is relevant to notice that scleral imaging modalities differ among authors, which could bias the estimation of AST and, consequently, the associated variables. Most of these investigations use spectral domain optical coherence tomography combined with the enhanced depth imaging technique [28] or an anterior module to obtain sclera in vivo images. However, the swept-source technology (SS-OCT) uses longer wavelengths, thereby enabling faster scanning speed, greater sensitivity, less light scattering, and deeper structural resolution [29, 30]; however, it was only used by a few due to its recent emergence on the medical market.

Enhancing knowledge on AST measurements by advanced imaging technics and their correlations with ocular variables is of particular importance given the association of scleral features with diseases such as open angle glaucoma [31], scleritis and episcleritis [32], and myopia [17]. Moreover, the characterization of the AST profile might help in the planning and monitoring of ophthalmological surgery, such as scleral-fixated intraocular lenses [33], trabeculectomies [34], intravitreal injections, and glaucoma, as well as in monitoring the effect of glaucoma medical treatment [35]. Finally, the association of biomechanical corneal metrics with AST may be beneficial to better understand the implication of the sclera on corneal response, given its relevant role in the early diagnosis of keratoconus [9, 10], planning the type of refractive surgery and monitoring procedures that modify the scleral tissue, such as myopia progression and prostaglandin treatment in glaucoma. Hence, the purpose of the current study was to measure the AST at different scleral eccentricities across several meridians using swept-source technology, to evaluate its association with ocular parameters in order to estimate the relationship between the biomechanical corneal response and AST.

Methods

A cross-sectional prospective nonrandomized study was carried out at the FISABIO-Oftalmología Médica (FOM) from January 2020 to March 2020. The approval of the institutional Ethics Committee (V1 1-04-2019) was acquired prior to the start, and it was conducted in accordance with the tenets of the Declaration of Helsinki. All participants provided a written informed consent.

Patients

Sixty healthy eyes from 60 Caucasian patients aged between 18 and 45 years were recruited from the FOM and the Faculty of Optics and Optometry from the University of Valencia, Valencia,

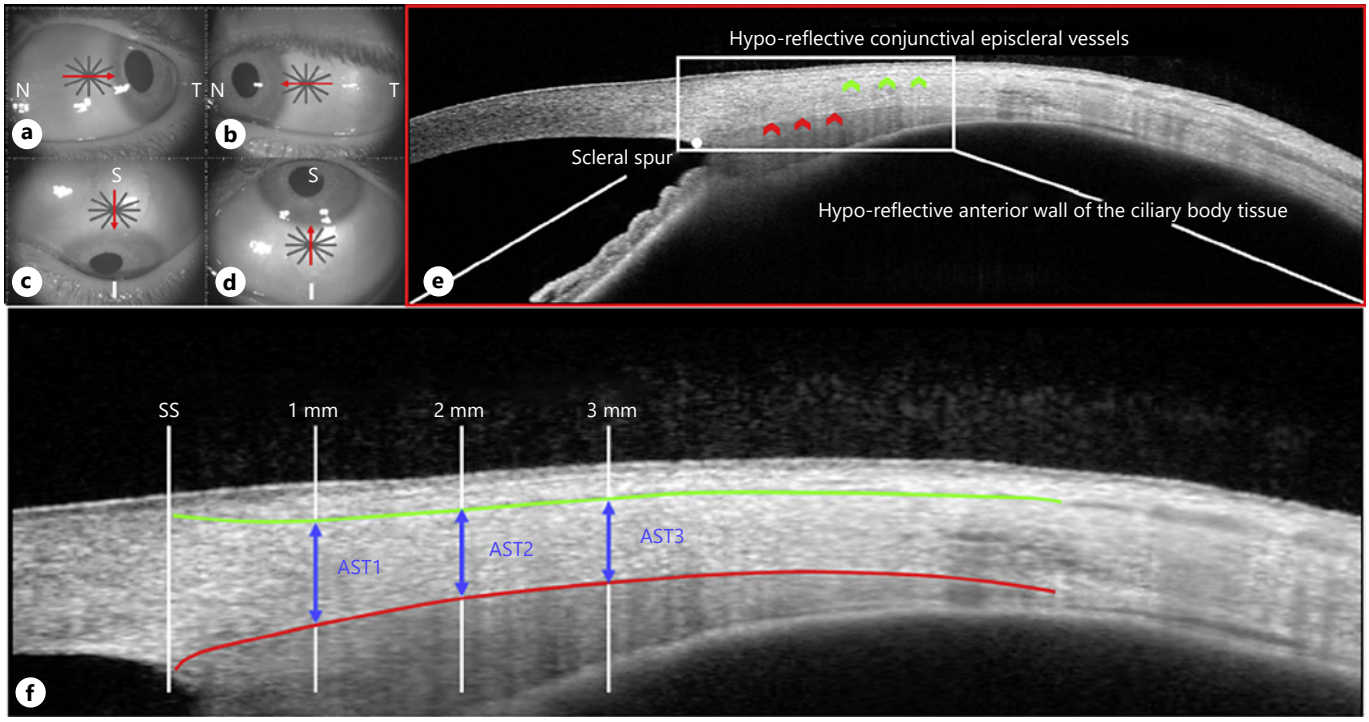

Color version available online

Fig. 1. Illustration of the anterior en face OCT image of the scanning protocol used to perform the anterior scleral thickness (AST) quantification. **a–d** The red arrow represents the B-scan selected for (**a**) the nasal, (**b**) temporal, (**c**) superior, and (**d**) inferior meridians where the three main structures are marked (**e**): the scleral spur (SS) (white point), the outer boundary identified as the hypo-reflective conjunctival episcleral vessels (marked with green arrows), and the inner boundary identified as the hypo-reflective anterior wall of the ciliary body (marked with red arrows). **f** Sequential AST measurements, delimited by the anterior (green line) and posterior scleral wall (red line), were taken at 1, 2, and 3 mm (AST1, AST2, and AST3, respectively, blue arrows) locations posterior to the SS.

Spain, although finally only 50 eyes completed all the preliminary conditions. Five eyes were excluded due to misalignment during AST measurements as were five others that exhibited scattered images with lower axial resolution, therefore not allowing a clear AST estimation. Only one eye was randomly selected in each subject to avoid biased results of two eyes of the same patient.

All the subjects underwent a comprehensive ophthalmic examination prior to the OCT and biomechanical measurements. The same established study protocol was always followed, including subjective refraction, corrected distance visual acuity (CDVA), AL with an IOL Master 700 (Carl Zeiss Meditec, Jena, Germany), slit lamp biomicroscopy exam, and topography analysis with a Pentacam HR (Oculus Optikgeräte GmbH, Wetzlar, Germany). Three measurements were taken with each device by the same qualified expert to avoid inaccurate values and that of the highest quality was selected for further analysis as recommended by the manufacturers.

The inclusion criteria were age greater than 18 years, spherical equivalent (SE) up to ±6 diopters (D), BCVA better than 0.00 logMAR, AL greater or equal to 22 mm, and AL less or equal to 26 mm given its relationship with scleral thickness [19, 20]. None of the participants had clinical signs on slit lamp (corneal thinning, anterior corneal scar, or epithelial staining) that could modify the biomechanical parameters. Patients with an asymmetric pattern in corneal topography, previous refractive surgery, any history of ocular trauma or corneal diseases, or the use of contact lenses and topical medications at least 2 weeks before the exploration were excluded from the study.

Experimental Procedure

The experimental procedure was performed after the initial screening of all participants. The exploration of each subject was conducted on a single day. The biomechanical and AST measurements were carried out in random order after a period of washout between both devices. The measurement session was planned in the afternoon, and the timing was scheduled between 3:00 p.m. and 7:00 p.m. to avoid the possible effects of diurnal variations of AST [25].

Biomechanical Measurements

Biomechanical parameters were measured using a noncontact tonometer (Corvis ST; Oculus Optikgeräte GmbH, Wetzlar, Germany). The device monitors the response of the cornea to an air pressure pulse using an ultra-high-speed Scheimpflug camera that captures 140 images at a frame rate of 4,430 Hz. The cornea undergoes three main stages; the first applanation is an ingoing phase until it achieves the highest concavity (second stage) and a returning phase when the cornea goes through the second applanation

[36]. The dynamic corneal response parameters were reported by the software analysis and exported for each exam. The subset of dynamic corneal responses selected for further statistical analysis was length and speed of first (LA1, SA1) and second (LA2, SA2) applanation, deformation amplitude, distance between bending points or peak distance, concave radius of curvature at the highest concavity point, IOP, and CCT. Patients who did not present a quality score "*ok*" were excluded from the study.

AST Measurements

Scleral Imaging

The AST was analyzed across four scleral zones (nasal, temporal, superior, and inferior meridian) using the Casia 2 (AS SS-OCT; Tomey, Nagoya, Japan). This device is based on Fourier domain technology, and it uses a 1,310-nm wavelength swept-source laser at a frequency of 0.3 s to capture images with a scanning speed of 50,000 A-scan/second, 10-μm axial resolution, and 30-μm transverse resolution of the ocular tissue. The scan dimensions are 16 mm (width) × 16 mm (length) × 13 mm (depth).

The anterior global scan method was used for all image acquisition which consists of a radial scan of 16 cross-sectional images averaged from 128 images with a scan resolution of 800 A-scan, a resolution image of 800 × 11,000 PPI per line sampling, and a depth of 6 mm. The device uses automatic tracking technology to provide en face images and to track the eye in real time to improve the contrast and definition scan [30]. Three measurements were taken for each quadrant by the same examiner following a blind technique, and the mean of the values obtained was used for further analysis.

During imaging, all patients fixated on a nonaccommodative external target for a maximum of 3 s maintaining their chin positioned on the chin rest. The target was placed at 2 m of distance to control the AST variations with accommodation [22] and about 20° out off-axis at different regions to ensure the scan consistency over the same anterior scleral region. Attention to accuracy was taken to measure close to the limbus zone and to place one line from radial scan aligned upon the sclerocorneal reflex, while the examiner was looking at a real-time image of the patient's eye on the video monitor. Depending on the scleral meridian explored, the OCT cross-sectional image selected was modified to include the iris and to distinguish all the structures. The horizontal line scan (180°) was selected for the nasal and temporal meridians (shown in Fig. 1a, b), whereas the vertical line sampling (90°) was used for the superior and inferior meridians (shown in Fig. 1c, d). Lid retraction was necessary for inferior and vertical gaze in order to expose a large area of the sclera.

Data Analysis

The AST was measured on the same instrument without exporting the images to maintain the resolution. The Casia device applies paraxial calculation to calculate the corneal parameters using the refractive index of a Gullstrand's eye model (cornea = 1.376, aqueous humor = 1.336). Hence for convenience, a scleral refractive index of 1.376 was assumed, and the possible interface optical distortion produced by the different refractive indices of the anterior segment structures and the index layer variations was not corrected [37] like most of previous AST studies [17, 18, 21, 22, 25–27, 38].

On the B-scan selected from the 2D anterior segment analysis, the examiner marked the location of the scleral spur (SS) as a depressed zone near the limbal region. The outer scleral boundary was identified as the hypo-reflective conjunctival episcleral vessels, and the inner boundary as the hypo-reflective anterior wall of ciliary body tissue (shown in Fig. 1d). The AST was quantified manually with calipers at the distance between both walls. The calipers' orientation and separation were placed tangential to the reflective scleral interfaces for better accuracy. The SS plane was the baseline point to achieve three consecutive measurements every 1 mm (AST1, AST2, AST3) (shown in Fig. 1f) in order to (1) evaluate if AST varies posterior to the SS across each meridian; (2) obtain a consistent average of each region; (3) test if the association between AST and the corneal response parameters could change according to the evaluated meridian. If a scattered OCT image was observed that did not allow a clear sighting of the scleral structure, the patient was excluded from the study.

Statistical Analysis

All statistical analyses were performed using SPSS software version 26.0 (Chicago, IL, USA) for Mac OS. The normality of distribution was verified using the Kolmogorov-Smirnov normality test.

A two-way repeated measures ANOVA was conducted to assess if there were any AST differences throughout scleral eccentricity (i.e., between 1, 2, and 3 mm, three levels) and scleral region (i.e., between nasal, temporal, superior, and inferior, four levels) and to explore the interaction between eccentricity and region. In all cases, post hoc analysis with Bonferroni adjustment was conducted if Mauchly's sphericity test was not violated (p value >0.05). If not, the assumption of sphericity was not met and was calculated according to Greenhouse and Geisser [39] to correct the repeated measures ANOVA. The intraclass correlation coefficient two-way mixed effects with absolute agreement model were used to estimate the intra-observer agreement in AST measurements.

To reduce the large set of biomechanical variables included in the study, a principal component analysis (PCA) was used to create new components which account for most of the variance in the original biomechanical variables. Multiple linear regression analysis was performed to investigate both, the association between AST and several factors, and the association of the new biomechanical components with AST over each scleral region. In both cases, p values (2-tailed) < 0.05 were considered statistically significant.

Results

The study comprised a total of 50 healthy eyes of 50 patients. The mean age was 29.02 ± 9.58 years. The mean SE error and AL were −1.04 ± 1.51 D and 23.74 ± 1.00 mm, respectively. Table 1 summarizes the demographic and ocular data of all participants.

The AST values are illustrated in Table 2 and Figure 2. The reproducibility of AST values between sessions revealed excellent intra-observer agreement (intraclass correlation coefficient ≥ 0.98 in all eccentricities and meridians, IC 0.97–0.99, $p < 0.001$). The AST exhibited its minimum thickness 2 mm posterior to the SS along the

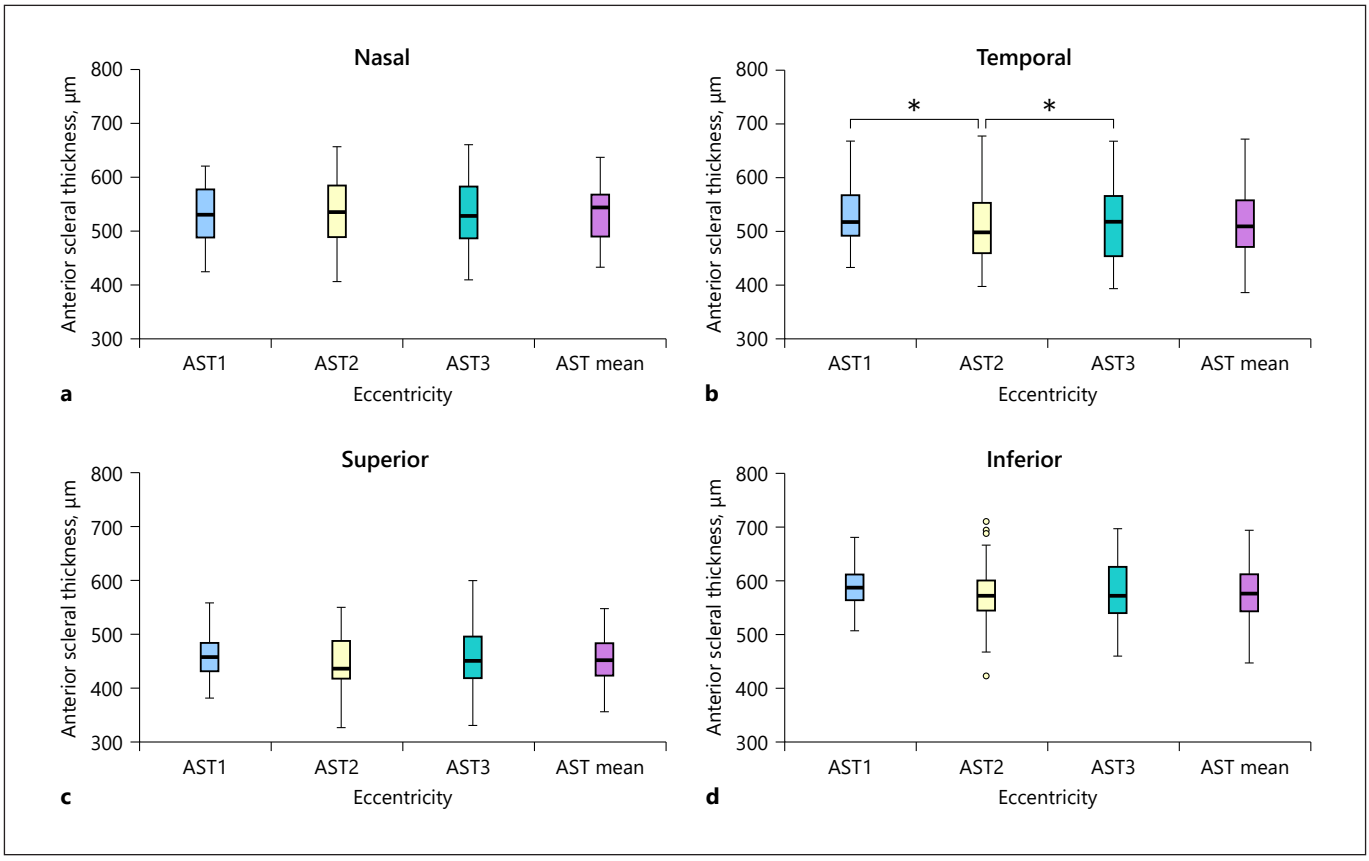

Fig. 2. Box plot of the AST profile (n = 50 eyes) over the four scleral regions evaluated. The nasal (**a**), temporal (**b**), superior (**c**), and inferior (**d**) meridians across the three scleral eccentricities from the scleral spur toward the periphery (AST1, AST2, and AST3) and the averaged AST value (AST mean). *A bold asterisk indicates the significant differences obtained from the two-way ANOVA repeated measurement analysis when post hoc analysis with Bonferroni adjustment was conducted for pairwise eccentricity comparisons.

Table 1. Summary of the demographic and ocular data of the 50 participants (50 eyes/50 patients)

Parameter	Mean ± SD (range)
Gender (female), *n* (%)	36 (72)
Ethnicity: Caucasian, *n* (%)	50 (100)
Age, years	29±9.58 (18–45)
SE, D	−1.04±1.51 (−5.63 to +1.88)
LogMAR CDVA	−0.05±0.06
AL, mm	23.74±1 (22–25.83)
IOP, mm Hg	14.54±2.01 (10.5–19.50)
CCT, µm	540±30.83 (481–605)

Categorical variables are reported as *n* (%) and continuous variables as mean ± SD (range). SE, spherical equivalent; D, diopters; CDVA, corrected distance visual acuity; AL, axial length; IOP, intraocular pressure; CCT, central corneal thickness; SD, standard deviation.

Table 2. AST (mean ± standard deviation (SD), µm) at 1 (AST1), 2 (AST2), and 3 (AST3) mm posterior to the SS across the four scleral meridians explored

Scleral region	AST (mean ± SD, µm)			
	AST1	AST2	AST3	AST mean
Nasal	525±51	531±58	532±65	529±53
Temporal	522±65	497±63	513±71	511±59
Superior	457±43	448±48	453±53	441±42
Inferior	587±53	578±57	580±59	581±52

AST mean represents the averaged value of the three measurements.

Table 3. Multivariate linear regression analysis for anterior scleral thickness (AST) with an adjusted model for scleral region, spherical equivalent (SE), age, gender, axial length (AL), central corneal thickness (CCT), and intraocular pressure (IOP)

Dependent variable	Independent variables		B coefficient (SD error)	95% confidence interval		*p* value
				lower	upper	
AST R^2 adjusted = 0.45	Intercept		110.48 (51.88)	8.639	212.323	0.034
	Region	Inferior	131.59 (5.60)	120.60	142.59	<0.001
		Nasal	80.95 (5.57)	70.02	91.89	<0.001
		Temporal	57.63 (5.57)	46.70	68.57	<0.001
		Superior	†			
	AL		9.50 (2.05)	5.47	13.53	<0.001
	CCT		0.27 (0.07)	0.13	0.41	<0.001
	IOP		−2.25 (1.01)	−4.22	−0.26	0.026

† Reference value considered to compare within the four scleral regions.

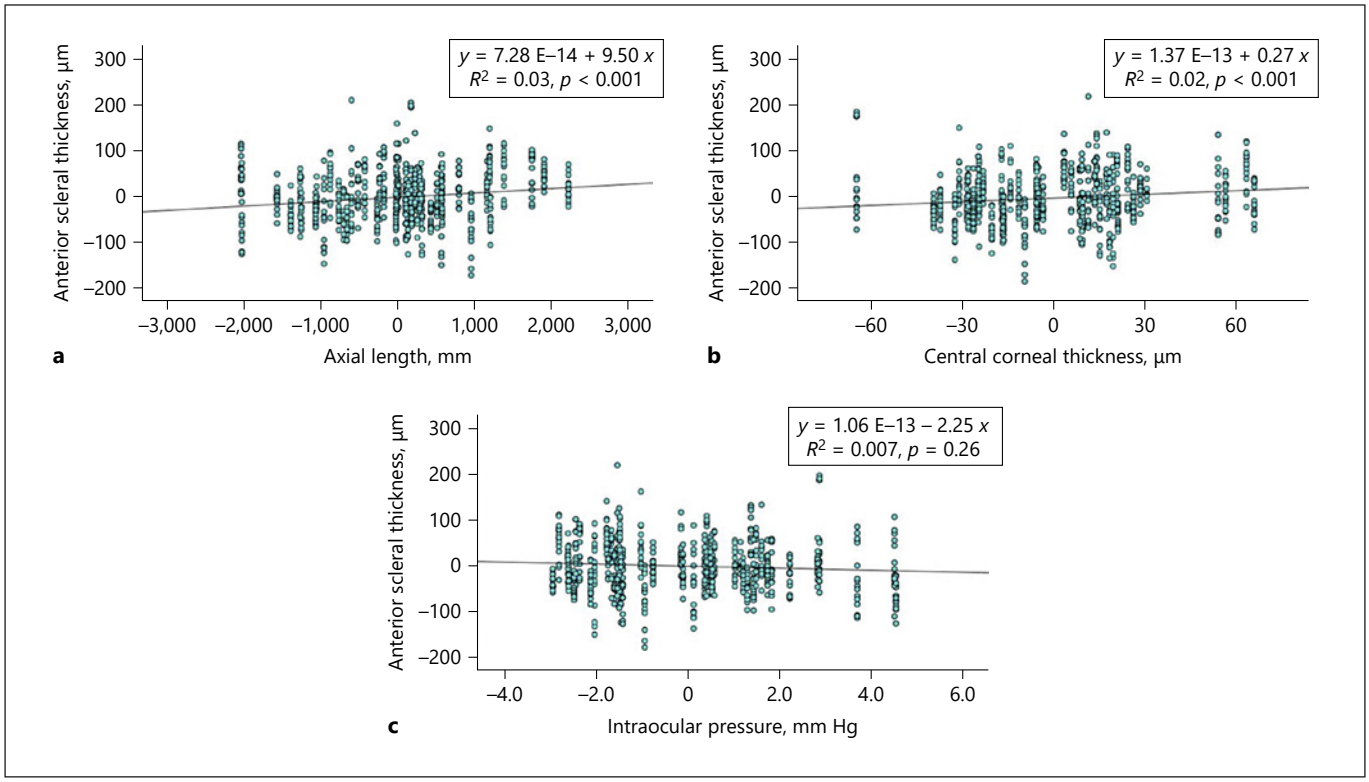

Fig. 3. Partial scatterplot representing the linear regression between the AST and the AL (**a**), CCT (**b**), and IOP (**c**). The upper right box represents the linear regression equation, the linear R^2, and the *p* value.

temporal, superior, and inferior meridians, whereas the nasal meridian toward the 1 mm location. On average, the sclera was significantly thicker at the inferior meridian compared to the nasal, temporal, and the superior meridian ($p < 0.001$, at all eccentricities), and significantly thinner at superior meridian compared to all regions ($p < 0.001$, at all eccentricities). The results of the two-way repeated measures ANOVA revealed that there was signifi-

Table 4. Results of the principal component analysis (PCA) for the biomechanical parameters related to the inward (LA1, SA1), backward (LA2, SA2) moment, and maximum concavity (DA, PD, R) of the corneal response

Principal components	Rotated component matrix†							Total of variance explained Extraction sum of squared loadings		
	LA1	SA1	LA2	SA2	DA	PD	*R*	total	variance, %	cumulative, %
C1	−0.001	0.82	−0.15	−0.90	0.95	0.88	−0.47	3.77	53.84	53.84
C2	0.81	−0.36	0.67	0.14	−0.15	−0.02	0.52	1.16	16.51	70.34

C1 and C2 represent the new components that explain a cumulative 70.34% of the total amount of variance. LA1, length of first applanation; SA1, speed of first applanation; LA2, length of second applanation; SA2, speed of second applanation; DA, deformation amplitude; PD, distance between bending points, peak distance; *R*, radius; C1, component 1; C2, component 2. † The rotation method used was varimax with Kaiser normalization converged in 3 iterations.

Table 5. Multivariate linear regression analysis for the two new biomechanical components extracted using the PCA, C1 and C2, with an adjusted model for age, gender, spherical equivalent (SE), central corneal thickness (CCT), intraocular pressure (IOP), and anterior scleral thickness (AST) at the four meridians explored (nasal, temporal, superior, and inferior)

Dependent variable	Independent variables		B coefficient (SD error)	95% confidence interval		*p* value
				lower	upper	
C1 R^2 adjusted = 0.76	Intercept		5.76 (0.21)	5.33	6.19	<0.001
	IOP		−0.38 (0.009)	−0.40	−0.36	<0.001
	SE		−0.18 (0.01)	−0.21	−0.16	<0.001
	Age		0.02 (0.003)	0.016	0.026	<0.001
	Gender	Men	−0.224 (0.04)	−0.30	−0.15	<0.001
		Women	†			
	AST	Inferior	−0.002 (0)	−0.004	−0.001	<0.001
		Nasal	−0.004 (0.001)	−0.005	−0.002	0.046
		Temporal	−0.001 (0.001)	−0.002	0.00	0.043
		Superior	−0.002 (0.001)	−0.004	0.00	0.026
C2 R^2 adjusted = 0.174	Intercept		−5.66 (0.63)	−6.91	−4.42	<0.001
	CCT		0.09 (0.001)	−0.006	0.01	<0.001
	SE		−0.14 (0.02)	−0.181	−0.092	<0.001
	IOP		0.08 (0.02)	0.045	0.113	<0.001
	AST		−0.001 (0)	−0.002	−0.00	0.085
	Age		0.007 (0.005)	−0.003	0.016	0.155

A bold cross (†) represents the reference value considered to compare between men and women.

cant main effect of eccentricity ($F(1.44, 69) = 3.7$, $p = 0.044$, $\eta p^2 = 0.07$) and region ($F(3, 144) = 78.01$, $p = 0.000$, $\eta p^2 = 0.619$) on AST. Moreover, there was a significant interaction between eccentricity and scleral region ($F(4.5, 215.5) = 2.60$, $p = 0.03$, $\eta p^2 = 0.05$). The multivariate analysis adjusted for several parameters demonstrated that AST could be significantly associated with region, AL, CCT, and IOP (shown in Table 3; Fig. 3).

The PCA results showed that two components (component 1 [C1] and component 2 [C2]), which account for

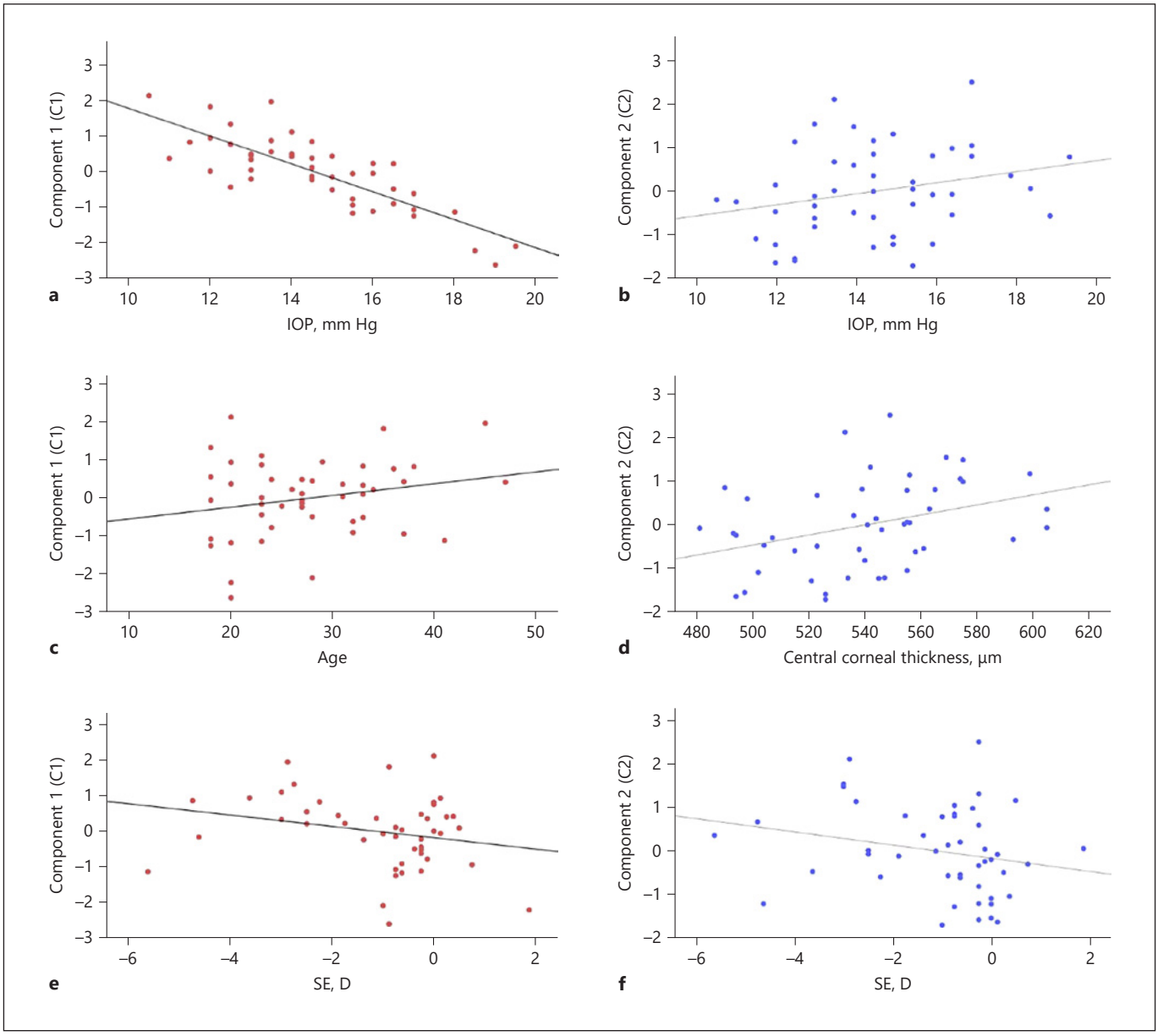

Color version available online

Fig. 4. Scatterplot representing the linear relationship between the two new principal components (C1, red dots and C2, blue dots) of the biomechanical corneal response with IOP (**a**, **b**), age (**c**), CCT (**d**), and SE (**e**, **f**). IOP, intraocular pressure; SE, spherical equivalent; C1, component 1; C2, component 2.

a cumulative 70.34% of the original biomechanical data set variability, have been extracted. C1 accounts for 53.84%, whereas C2 for the 16.51% of the total variance. The component matrix illustrated in Table 4 represents the coefficient weights extracted of each biomechanical parameter and the metrics that are mostly associated with the C1 and C2 models. Kaiser-Meyer-Olkin measure of sampling adequacy was 0.751, and Bartlett's test of sphericity was statistically significant ($p < 0.001$).

Multivariate regression models for both components are illustrated in Table 5 and Figure 4. The multivariate analysis highlighted that C1 was significantly linked with IOP, SE, age, gender, and AST over all regions ($p < 0.001$). C2 model was significantly associated with SE, CCT, and IOP ($p < 0.001$). Regarding AST, the model performed with C1 confirmed a negative and significative relationship over all meridians. The partial correlation adjusted for factors such as AL, CCT, IOP, gender, age, and SE

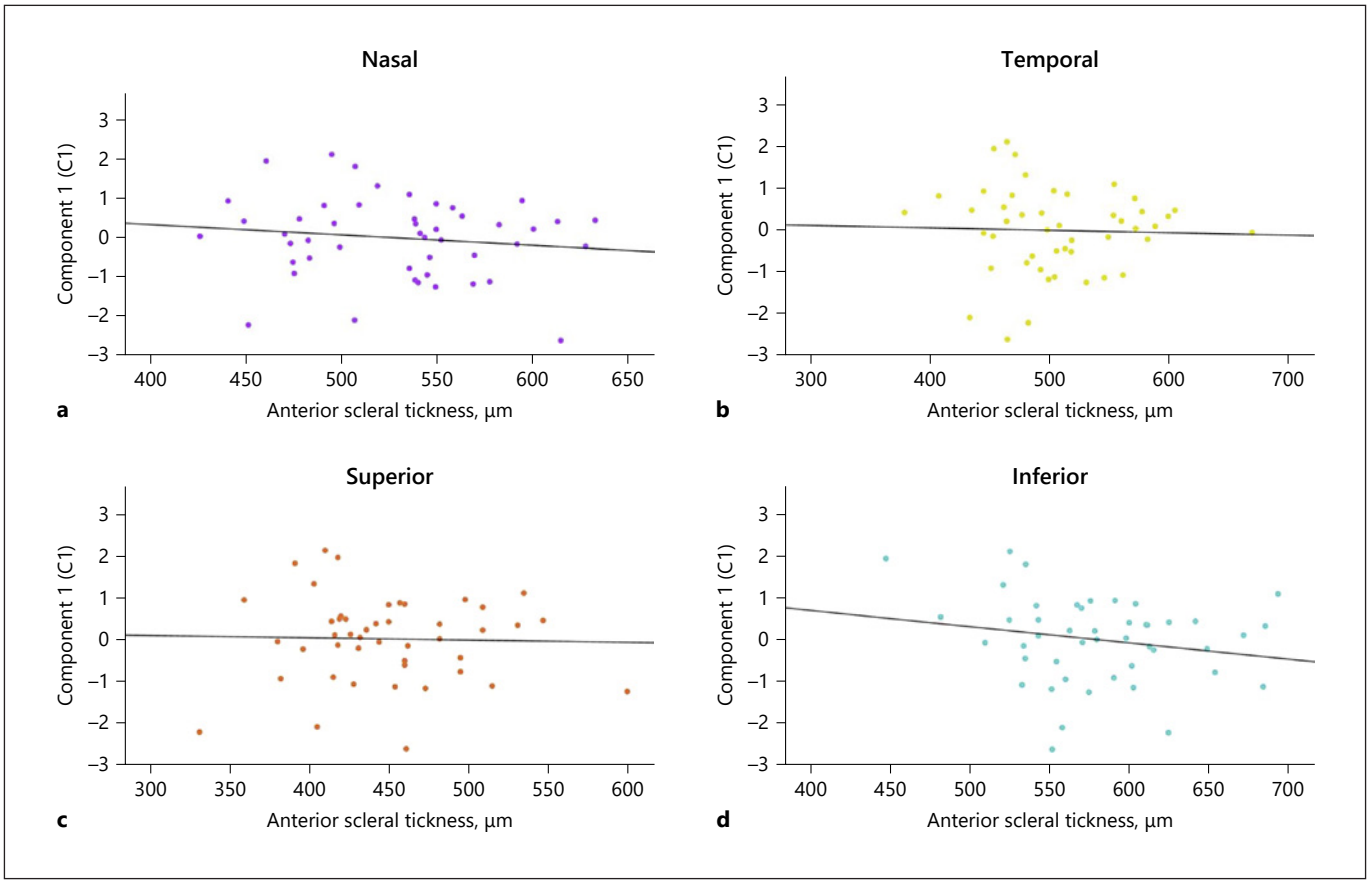

Color version available online

Fig. 5. Scatterplot representing the linear relationship between anterior scleral thickness (AST) and the new component (C1) of the biomechanical corneal response along the four scleral meridians: nasal (**a**), temporal (**b**), superior (**c**), and inferior (**d**). C1, component 1.

demonstrated a moderate and significative relationship over the nasal ($r = -0.36$, $p < 0.0001$, shown in Fig. 5a) and inferior meridians ($r = -0.26$, $p = 0.004$, shown in Fig. 5d), whereas there was a weak relationship over the temporal ($r = -0.14$, $p = 0.05$, shown in Fig. 5b) and superior meridians ($r = -0.15$, $p = 0.05$, shown in Fig. 5e).

Discussion

This study reports the in vivo AST profile of several scleral meridians and how the biomechanical corneal response and some ocular parameters are correlated with the AST. The results provide the first evidence that scleral thickness is associated with the biomechanical corneal response metrics. The current study also demonstrates that significant meridional variances in scleral thickness occur and prove that AST is associated with AL, CCT, and IOP.

The findings of this study show that over all meridians, the sclera was thicker in the inferior and thinner in the superior region; however, the scleral profile was similar across the nasal and temporal meridians. These results were generally consistent with the averaged results reported by Dhakal et al. [17] and those of Fernandez-Vigo et al. [27] who also used swept-source technology to determine the AST. By contrast, Sung et al. [18] obtained thicker values in all the meridians, but this was due to the inclusion of the episcleral vascular plexus, as Buckhurst et al. [38] who used a temporal domain OCT that had lower axial (18-µm) and transversal (60-µm) resolution than SS-OCT. Furthermore, Schlatter et al. [24] reported thinner values because they measured along the diagonal meridians and just 2 mm posterior to the SS.

These meridional variations have been associated with hypoxia phenomena of the unexposed sclera, which generate an increase in blood flow [40], with the asymmetrical expansion of the ocular globe inferior more than superior

[17] and also with the complexities of scleral biomechanics [18]. However, although the superior zone was also unexposed, thinner values were observed and no hypothesis has been found that suggests it might be as a result of inward pressure of the upper lid that produces a mechanical and frictional pressure. Considering that the shearing forces induced by blinking alters the migration and turnover of epithelial corneal cells [41] and the static upper eyelid pressure [42, 43]; hence, a possible redistribution of scleral collagen fiber may exist. Moreover, during eye movement, the force transmission from the ocular muscles to the sclera by Tenon's capsule could lead to a thin thickness [1].

Our outcomes demonstrate that AST variations with scleral eccentricity occurred, which were significantly only over the temporal region. Several authors [17, 18, 25–27, 38] reported that scleral thickness decreased significantly from the SS region toward the scleral equator for all meridians. However, it could be reasonable to find a small disparity considering that the present study analyzes the AST without taking into account the diversity of refractive error (emmetropes, $n = 30$, SE range = +0.75 to −0.75 D, mild myopes, $n = 16$, SE range = −1.0 to −3.0 D and moderate myopes, $n = 4$, SE range = −3.0 to −6.0 D).

The AST was positively associated with the AL, and it could be contrary to evidence in the recent literature. However, Vurgese et al. [44] showed that in nonaxially elongated eyes (AL ≤26 mm, like the current study), the AST was not significantly associated with AL and higher scleral volume [45]. Moreover, the correlation was positive at the scleral equator as other authors have also described [21, 24, 26, 38]. A thicker AST yielded to a greater CCT which was consistent with certain studies [18, 26] but contrary to others [21, 38, 44] which described a null relationship. A thinner AST was related to a greater IOP; however, Fernández-Vigo et al. [27] described null relationship, whereas Sung et al. [18] reported that the negative association has exhibited significance by chance. However, Kling and Marcos [16] proved that as IOP increased, the wall tension increased in the cornea and sclera according to Laplace's law and both tissues became stiffer due to the nonlinear material properties. Therefore, it was to be expected that a thinner sclera stiffened to a lesser extent than thicker sclera, and consequently, IOP presented higher values because the scleral wall tension was reduced. Even so, due to the divergence in the analysis of the scleral imaging technology and the complexity of scleral tissue, further investigations are required to conclude and generalize the association between AST, CCT, and IOP. AST is not correlated with the refractive error according to previous reports [18, 26, 27, 38, 44]. However, although Dhakal et al. [17] reported an AST decrease with an increasing degree of myopic SE only in the inferior meridian, the inclusion of a wide range of myopes compared to the present study could explain these differences. Our results showed that gender and age were not factors associated with AST. However, controversial results can be found about their relationship with AST in the literature [18, 21, 25–27, 38, 44].

The results of the current study also aimed to investigate how the corneal biomechanical response could be linked to different ocular factors. It has been widely reported that the IOP is the best predictor of the corneal response [16] which is in consistent with the linear model made with C1. However, in the C2 model, the corneal response was mostly related to the CCT. These findings were confirmed by previous studies, which demonstrated that IOP and pachymetry bear a considerable influence on most corneal biomechanical parameters provided by the Corvis ST [8, 14–16].

Our study only demonstrated that women presented a greater corneal response (female-to-male ratio, 36:14) in the C1 model. However, currently, there have been a few studies in which the association between gender and corneal response has been evaluated. Strobbe et al. [46] described that the viscosity and elastic corneal properties were higher in Caucasian men and with advancing age. Moreover, it has been observed that the mechanical response decreased with advancing age as previously described by other investigators [14, 15]. Interestingly, refractive error was correlated with both components, C1 and C2. Most corneal biomechanical metrics increase in myopic eyes which means that the tissue resistance becomes weaker. These findings agree with some reports which demonstrate that the elastic properties of the cornea are less compliant in myopic eyes, especially in high myopia, compared to emmetropic and hyperopic eyes where a stiffer biomechanical corneal response was observed [47, 48].

During an air puff pulse, when the cornea goes through the highest concavity state, a fluid displacement in the anterior chamber occurs and the stress transmitted to the scleral wall produces a corneal response alteration in which scleral stiffness takes part [11–13]. Our results confirm that the AST was significantly associated with the corneal response along the four scleral meridians in C1. This association was greater over the nasal and inferior meridians compared to the temporal and superior meridians. A greater AST yielded to a slight limitation of the corneal response. However, C2 did not show any association with AST. It should be noted that C1 was mainly

constructed with biomechanical parameters coming from the highest concavity state (deformation amplitude and peak distance) and the ingoing (SA1) and returning (SA2) speed of the corneal tissue, whereas the C2 model was mainly constructed by the metrics of the applanation length in the loading (LA1) and unloading (LA2) phase. The study by Nguyen et al. [12] suggests that the parameters obtained from the first applanation would be less sensitive to scleral properties and just characteristic of corneal properties, which might explain why C1 showed greater association with AST than C2. It is therefore possible that the mechanical anisotropy, which varies with the scleral anatomical position [1], the scleral tissue water content [2], the asymmetrical patterns of the collagen over the globe [5], might explain the different meridional associations between C1 and the four scleral meridians that were analyzed. Despite this, the significant results need further investigations due to the small change in the corneal response with AST to enhance the knowledge of the role of AST in the corneal response.

The current study has some limitations. First, the optical distortion produced by the different refractive index layers was not corrected [37] because the effect was expected to be minimal due to the small difference (0.03) between the conjunctiva (1.41) and the sclera (1.38). In addition, several studies did not consider this factor in their calculations [17, 18, 21, 22, 25–27, 38]. Second, the thickness measurement could be biased by B-scan rotation/tilt and image curvature. Alonso-Caneiro et al. [49] described an induced error in the AST estimation without considering the Laplace correction and tilt in their calculations. However, the thickness adjustment was not performed in most of the AST studies. Additional limitations are the diversity of the refractive error and the small sample size, which could strengthen the present findings.

Conclusions

The AST was thickest in the inferior region and thinnest in the superior when compared to any other meridian which supports the hypothesis of the asymmetrical global expansion of the ocular globe (greater along the superior-inferior meridian in comparison with the nasotemporal meridian). The horizontal meridian did not show any significant thickness modification. These outcomes prove that significant thickness variations in the scleral region, AL, CCT, and IOP occurred, while age, gender, and refractive error were factors that were not associated with the scleral thickness. These findings also demonstrate that the corneal biomechanical response is significantly correlated with IOP, CCT, SE, gender, age, and, in a lesser proportion, with AST along the four scleral regions explored. In this context, although the association varied between meridians, the relation was moderate over the nasal and inferior meridians and weak over the temporal and superior meridians. This is the first evidence regarding the link with the AST to corneal biomechanical parameters. The AST association was especially with the biomechanical metrics related to the highest concavity moment and the speed of the ingoing and outgoing phase. Further investigation is required to generalize the findings of the current study.

Acknowledgments

We would like to thank the Cathedra Alcon-FISABIO-UVEG for its support and also Marylin Noyes for the manuscript revision.

Statement of Ethics

This cross-sectional prospective study was approved by the institutional Ethics Committee of FISABIO-Oftalmología Médica (FOM) (V1 1-04-2019), and it was conducted in accordance with the tenets of the Declaration of Helsinki. All participants provided a written informed consent prior to the study involvement.

Conflict of Interest Statement

The authors have no conflicts of interest to declare regarding the instruments or materials mentioned in this article.

Funding Sources

No funding, public or private, was received.

Author Contributions

Neus Burguera-Giménez designed the study, collected and analyzed the data, and took the writing lead. Mª Amparo Díez-Ajenjo designed the study, analyzed the data, and edited and supervised the manuscript. Noemí Burguera and Mª José Luque-Cobija analyzed the data and edited the manuscript. Cristina Peris Martínez designed and directed the study. All the authors discussed the results, reviewed the manuscript, and agreed to the published version of the manuscript.

Data Availability Statement

Data are available on request due to data protection. Further inquiries can be directed to the corresponding author.

References

1 Boote C, Sigal IA, Grytz R, Hua Y, Nguyen TD, Girard MJA. Scleral structure and biomechanics. Prog Retin Eye Res. 2020;74:100773.
2 Summers Rada JA, Shelton S, Norton TT. The sclera and myopia. Exp Eye Res. 2006 Feb;82(2):185–200.
3 Kain SR. Methods and protocols. Methods Biochem Anal. 2005;47:407–21.
4 Yang B, Jan NJ, Brazile B, Voorhees A, Lathrop KL, Sigal IA. Polarized light microscopy for 3-dimensional mapping of collagen fiber architecture in ocular tissues. J Biophotonics. 2018;11(8):e201700356.
5 Gogola A, Jan NJ, Brazile B, Lam P, Lathrop KL, Chan KC, et al. Spatial patterns and age-related changes of the collagen crimp in the human cornea and sclera. Invest Ophthalmol Vis Sci. 2018;59(7):2987–98.
6 Liu J, Roberts CJ. Influence of corneal biomechanical properties on intraocular pressure measurement: quantitative analysis. J Cataract Refract Surg. 2005;31(1):146–55.
7 Pepose JS, Feigenbaum SK, Qazi MA, Sanderson JP, Roberts CJ. Changes in corneal biomechanics and intraocular pressure following LASIK using static, dynamic, and noncontact tonometry. Am J Ophthalmol. 2007;143(1):39–47.
8 Broman AT, Congdon NG, Bandeen-Roche K, Quigley HA. Influence of corneal structure, corneal responsiveness, and other ocular parameters on tonometric measurement of intraocular pressure. J Glaucoma. 2007;16(7):581–8.
9 Vinciguerra R, Ambrósio R, Elsheikh A, Roberts CJ, Lopes B, Morenghi E, et al. Detection of keratoconus with a new biomechanical index. J Refract Surg. 2016;32(12):803–10.
10 Ferreira-Mendes J, Lopes BT, Faria-Correia F, Salomão MQ, Rodrigues-Barros S, Ambrósio R. Enhanced ectasia detection using corneal tomography and biomechanics. Am J Ophthalmol. 2019;197:7–16.
11 Metzler KM, Mahmoud AM, Liu J, Roberts CJ. Deformation response of paired donor corneas to an air puff: Intact whole globe versus mounted corneoscleral rim. J Cataract Refract Surg. 2014;40(6):888–96.
12 Nguyen BA, Reilly MA, Roberts CJ. Biomechanical contribution of the sclera to dynamic corneal response in air-puff induced deformation in human donor eyes. Exp Eye Res. 2020;191:107904.
13 Nguyen BA, Roberts CJ, Reilly MA. Biomechanical impact of the sclera on corneal deformation response to an air-puff: a finite-element study. Front Bioeng Biotechnol. 2019;6:1–8.
14 Vinciguerra R, Elsheikh A, Roberts CJ, Ambrósio R, Kang DSY, Lopes BT, et al. Influence of pachymetry and intraocular pressure on dynamic corneal response parameters in healthy patients. J Refract Surg. 2016 Aug;32(8):550–61.
15 Bao F, Deng M, Wang Q, Huang J, Yang J, Whitford C, et al. Evaluation of the relationship of corneal biomechanical metrics with physical intraocular pressure and central corneal thickness in ex vivo rabbit eye globes. Exp Eye Res. 2015 Aug;137:11–7.
16 Kling S, Marcos S. Contributing factors to corneal deformation in air puff measurements. Invest Ophthalmol Vis Sci. 2013 Jul;54(7):5078–85.
17 Dhakal R, Vupparaboina KK, Verkicharla PK. Anterior sclera undergoes thinning with increasing degree of myopia. Invest Ophthalmol Vis Sci. 2020;61(4):6.
18 Sung MS, Ji YS, Moon HS, Heo H, Park SW. Anterior scleral thickness in myopic eyes and its association with ocular parameters. Ophthalmic Res. 2021;64(4):567–76.
19 Jonas JB, Ohno-Matsui K, Holbach L, Panda-Jonas S. Association between axial length and horizontal and vertical globe diameters. Graefes Arch Clin Exp Ophthalmol. 2017;255(2):237–42.
20 Lee SM, Choi HJ, Choi H, Kim MK, Wee WR. Estimation of axial curvature of anterior sclera: correlation between axial length and anterior scleral curvature as affected by angle kappa. BMC Ophthalmol. 2016;16(1):176–11.
21 Oliveira C, Tello C, Liebmann J, Ritch R. Central corneal thickness is not related to anterior scleral thickness or axial length. J Glaucoma. 2006;15(3):190–4.
22 Woodman-Pieterse EC, Read SA, Collins MJ, Alonso-Caneiro D. Anterior scleral thickness changes with accommodation in myopes and emmetropes. Exp Eye Res. 2018;177:96–103.
23 Niyazmand H, Read SA, Atchison DA, Alonso-Caneiro D, Collins MJ. Anterior scleral thickness and shape changes with different levels of simulated convergence. Exp Eye Res. 2021 Feb;203:108435.
24 Schlatter B, Beck M, Frueh BE, Tappeiner C, Zinkernagel M. Evaluation of scleral and corneal thickness in keratoconus patients. J Cataract Refract Surg. 2015;41(5):1073–80.
25 Read SA, Alonso-Caneiro D, Free KA, Labuc-Spoors E, Leigh JK, Quirk CJ, et al. Diurnal variation of anterior scleral and conjunctival thickness. Ophthalmic Physiol Opt. 2016;36(3):279–89.
26 Read SA, Alonso-Caneiro D, Vincent SJ, Bremner A, Fothergill A, Ismail B, et al. Anterior eye tissue morphology: scleral and conjunctival thickness in children and young adults. Sci Rep. 2016;6:33796–10.
27 Fernández-Vigo JI, Shi H, Burgos-Blasco B, Fernández-Aragón S, De-Pablo-Gómez-de-Liaño L, Kudsieh B, et al. Anterior scleral thickness dimensions by swept-source optical coherence tomography. Clin Exp Optom. 2021 Jun;105(1):13–9.
28 Spaide RF, Koizumi H, Pozzoni MC, Pozonni MC. Enhanced depth imaging spectral-domain optical coherence tomography. Am J Ophthalmol. 2008;146(4):496–500.
29 Takusagawa HL, Hoguet A, Junk AK, Nouri-Mahdavi K, Radhakrishnan S, Chen TC. Swept-source OCT for evaluating the lamina cribrosa: a report by the American Academy of Ophthalmology. Ophthalmology. 2019;126(9):1315–23.
30 Radhakrishnan S, Rollins AM, Roth JE, Yazdanfar S, Westphal V, Bardenstein DS, et al. Real-time optical coherence tomography of the anterior segment at 1310 nm. Arch Ophthalmol. 2001 Aug;119(8):1179–85.
31 Yoo C, Eom YS, Suh Y-W, Kim YY. Central corneal thickness and anterior scleral thickness in Korean patients with open-angle glaucoma: an anterior segment optical coherence tomography study. J Glaucoma. 2011 Feb;20(2):95–9.
32 Shoughy SS, Jaroudi MO, Kozak I, Tabbara KF. Optical coherence tomography in the diagnosis of scleritis and episcleritis. Am J Ophthalmol. 2015 Jun;159(6):1045–9.e1.
33 Shahid SM, Flores-Sánchez BC, Chan EW, Anguita R, Ahmed SN, Wickham L, et al. Scleral-fixated intraocular lens implants-evolution of surgical techniques and future developments. Eye. 2021 Jun;35(11):2930–61.
34 Raj A, Bahadur H. Morphological analysis of functional filtering blebs with anterior segment optical coherence tomography: a short-term prediction for success of trabeculectomy. Eur J Ophthalmol. 2021 Jul;31(4):1978–85.
35 Park J-H, Yoo C, Chung HW, Kim YY. Effect of prostaglandin analogues on anterior scleral thickness and corneal thickness in patients with primary open-angle glaucoma. Sci Rep. 2021 Dec;11(1):11098.
36 Ambrósio Jr R, Ramos I, Luz A, Faria FC, Steinmueller A, Krug M, et al. Dynamic ultra high speed Scheimpflug imaging for assessing corneal biomechanical properties. Rev Bras Oftalmol. 2013 Apr;72(2):99–102.
37 Westphal V, Rollins A, Radhakrishnan S, Izatt J. Correction of geometric and refractive image distortions in optical coherence tomography applying Fermat's principle. Opt Express. 2002 May;10(9):397.
38 Buckhurst HD, Gilmartin B, Cubbidge RP, Logan NS. Measurement of scleral thickness in humans using anterior segment optical coherent tomography. PLoS One. 2015;10(7):e0132902–10.
39 Greenhouse SW, Geisser S. On methods in the analysis of profile data. Psychometrika. 1959;24(2):95–112.
40 Efron N, Carney LG. Oxygen levels beneath the closed eyelid. Invest Ophthalmol Vis Sci. 1979;18(1):93–5.

41 Mathers WD, Lemp MA. Morphology and movement of corneal surface cells in humans. Curr Eye Res. 1992 Jun;11(6):517–23.
42 Shaw AJ, Collins MJ, Davis BA, Carney LG. Eyelid pressure and contact with the ocular surface. Invest Ophthalmol Vis Sci. 2010; 51(4):1911–7.
43 Yamamoto Y, Shiraishi A, Sakane Y, Ohta K, Yamaguchi M, Ohashi Y. Involvement of eyelid pressure in lid-wiper epitheliopathy. Curr Eye Res. 2016;41(2):171–8.
44 Vurgese S, Panda-Jonas S, Jonas JB. Scleral thickness in human eyes. PLoS One. 2012 Jan; 7(1):e29692.
45 Jonas JB, Holbach L, Panda-Jonas S. Scleral cross section area and volume and axial length. PLoS One. 2014 Mar;9(3):e93551. Boote C, editor.
46 Strobbe E, Cellini M, Barbaresi U, Campos EC. Influence of age and gender on corneal biomechanical properties in a healthy Italian population. Cornea. 2014 Sep;33(9):968–72.
47 Bueno-Gimeno I, España-Gregori E, Gene-Sampedro A, Lanzagorta-Aresti A, Piñero-Llorens DP. Relationship among corneal biomechanics, refractive error, and axial length. Optom Vis Sci. 2014 May;91(5):507–13.
48 Radhakrishnan H, Miranda MA, O'donnell C. Corneal biomechanical properties and their correlates with refractive error. Clin Exp Optom. 2012 Jan;95(1):12–8.
49 Alonso-Caneiro D, Read SA, Vincent SJ, Collins MJ, Wojtkowski M. Tissue thickness calculation in ocular optical coherence tomography. Biomedical Optics Express. 2016 Feb; 7(2):629–45.